

Biasing and Genus Statistics of Dark Matter Halos in the Hubble Volume Simulation

Chiaki HIKAGE, Atsushi TARUYA and Yasushi SUTO

Department of Physics, School of Science, The University of Tokyo, Tokyo 113-0033

hikage@utap.phys.s.u-tokyo.ac.jp, ataruya@utap.phys.s.u-tokyo.ac.jp, suto@phys.s.u-tokyo.ac.jp

(Received 2002 February 9; accepted 2002 December 18)

Abstract

We present a numerical analysis of genus statistics for dark matter halo catalogs from the Hubble volume simulation. The huge box-size of the Hubble volume simulation enables us to carry out a reliable statistical analysis of the biasing properties of halos at a Gaussian smoothing scale of $R_G \geq 30h^{-1}\text{Mpc}$ with a cluster-mass scale of between $7 \times 10^{13}h^{-1}M_\odot$ and $6 \times 10^{15}h^{-1}M_\odot$. A detailed comparison of the genus for dark matter halos with that for the mass distribution shows that the non-Gaussianity induced by the halo biasing is comparable to that by nonlinear gravitational evolution, and both the shape and the amplitude of the genus are almost insensitive to the halo mass at $R_G \geq 30h^{-1}\text{Mpc}$. In order to characterize the biasing effect on the genus, we apply a perturbative formula developed by Matsubara (1994). We find that the perturbative formula well describes the simulated halo genus at $R_G \geq 50h^{-1}\text{Mpc}$. The result indicates that the biasing effect on the halo genus is well approximated by nonlinear deterministic biasing up to the second-order term in the mass density fluctuation. The two parameters describing the linear and quadratic terms in the nonlinear biasing accurately specify the genus for galaxy clusters.

Key words: cosmology: dark matter — cosmology: large-scale structure of universe — galaxies: clusters: general — galaxies: halos — methods: statistical

1. Introduction

The genus statistics characterizes the topological nature of a density field. In contrast to the more conventional two-point statistics, such as the two-point correlation functions or the power spectrum, the genus is sensitive to the phase information of a density field; therefore, the genus provides complementary information of the present cosmic structure. The genus has an analytic formula in a density field described by random-Gaussian statistics. Since Gott et al. (1986) proposed the genus of the large-scale structure as a test of the hypothesis that the initial perturbations are Gaussian, the genus has been evaluated for various galaxy or galaxy cluster catalogs (e.g., Gott et al. 1989; Park et al. 1992; Moore et al. 1992; Rhoads et al. 1994; Vogeley et al. 1994; Canavezes et al. 1998; Hoyle et al. 2002; Hikage et al. 2002). These investigations generally indicate consistency with the initial Gaussianity.

For a statistical analysis based on the distribution of *luminous* objects, however, non-Gaussianity produced in the process of cosmic structure formation should be properly considered. Gravitational nonlinear evolution is one of the most important non-Gaussian sources. It has been well studied using a variety of models, including a perturbative correction by the Edgeworth expansion (Matsubara 1994), direct numerical simulations (Matsubara, Suto 1996), an empirical lognormal model (Matsubara, Yokoyama 1996) and the Zel'dovich approximation (Seto et al. 1997).

Another non-Gaussian source is biasing, i.e., the sta-

tistical uncertainty between the spatial distribution of luminous objects and that of dark matter. Biasing is generally described by a nonlinear and stochastic function of the underlying mass density from various recent work (Dekel, Lahav 1999; Blanton et al. 1999; Somerville et al. 2001; Taruya et al. 2001). The difficulty in a general prediction of a biasing expression comes from the fact that the biasing properties are sensitive to the complicated formation mechanism of luminous objects. On the other hand, the biasing for dark matter halos, which are the most likely sites for galaxies and clusters, is relatively easy to be modeled and thus well investigated on the basis of both analytical and numerical approaches (Mo, White 1996; Taruya, Suto 2000; Yoshikawa et al. 2001). In particular, dark halos with cluster-scale mass are usually supposed to have a fairly good one-to-one correspondence with galaxy clusters, at least in a statistical sense. Therefore, biasing models for dark halos can be applied to upcoming galaxy cluster catalogs with an empirical relation between the halo mass and the temperature/luminosity of galaxy clusters (e.g., Kitayama, Suto 1997). In this spirit, Hikage et al. (2001) derives an analytical model of genus statistics for galaxy clusters with a nonlinear and stochastic halo biasing model of Taruya and Suto (2000).

A complementary approach to halo biasing is a direct analysis of cosmological numerical simulations. The statistical significance of previous studies, however, has been limited by the number of particles and the box-size employed in the simulations. Since the mean separation of rich clusters of galaxies is $\sim 50h^{-1}\text{Mpc}$, a typical cosmo-

logical simulation in a $300h^{-1}\text{Mpc}$ box has merely ~ 200 clusters. With this number of clusters, it is almost impossible to detect the cluster-mass dependence of various statistical measures in a reliable manner (e.g., Watanabe et al. 1994). This situation may be significantly improved by using the Hubble Volume Simulation (Jenkins et al. 2001). Specifically, we use the ΛCDM (Lambda Cold Dark Matter) data (AHVS, hereafter) at $z=0$, which employ $N=10^9$ particles in a box-size of $3h^{-1}\text{Gpc}$. The data enable us to quantitatively address the mass and scale dependence of the halo biasing and the related statistics.

In the present work, we perform a numerical analysis of the genus for dark halos with the Hubble volume simulation in order to clarify the uncertainty of the halo biasing in detecting the initial non-Gaussianity. From a detailed comparison between the genus for dark halos and that for dark matter, we find that the halo biasing effect on the non-Gaussianity of genus is comparable to the non-Gaussianity induced by the nonlinear gravitational evolution. In order to characterize the halo biasing effect on the genus statistics, we apply a perturbative formula developed by Matsubara (1994), and compare it with the simulated genus. We find that the perturbative formula properly describes the halo genus at a smoothing scale larger than $50h^{-1}\text{Mpc}$. Also, the biasing effect on the genus for halos is shown to be well-approximated by the nonlinear deterministic biasing up to the second-order terms in the mass density fluctuation.

The rest of the paper is organized as follows. We briefly describe the simulation data that we use and the halo catalogue in section 2. We then discuss in section 3 the biasing properties of dark halos while paying particular attention to their nonlinear and stochastic nature. We present a detailed study of the topology of the spatial distribution of dark halos using the genus statistics based on numerical simulations and a perturbative analysis in section 4. Finally section 5 is devoted to conclusions.

2. Dark Matter halos in the Hubble Volume Simulation

In the present work, we use the $z=0$ snapshot data of ΛCDM . The model assumes the density parameter of $\Omega_0=0.3$, cosmological constant of $\lambda_0=0.7$, and the Hubble constant in units of $100\text{km s}^{-1}\text{Mpc}^{-1}$, $h=0.7$. The fluctuation amplitude, smoothed over a top-hat radius of $8h^{-1}\text{Mpc}$, is set as $\sigma_8=0.9$ so that the model satisfies both the cluster abundance and the COBE normalization (e.g., Eke et al. 1996, Kitayama, Suto 1997). The initial density field is computed with CMBFAST assuming baryon density parameter of $\Omega_b h^2=0.0196$, and the random-Gaussian statistics (Colberg et al. 2000). The simulation box-size is $3000h^{-1}\text{Mpc}$ and the softening length for the gravitational force is set to be $100h^{-1}\text{kpc}$. An initial distribution of $N=10^9$ dark matter particles is generated using the Zel'dovich approximation, and is advanced with the Particle-Particle-Particle-Mesh (P^3M) code. The mass of each dark matter particle is set at $2.25 \times 10^{12} h^{-1} M_\odot$. Hamana et al. (2001) made sure that

the two-point clustering feature at $z=0$ in the AHVS is reliable even at an order of magnitude below the mean particle separation $3h^{-1}\text{Mpc}$ (still a few times larger than the adopted softening length). Thus, the dynamic range of the simulation data amounts to $\sim 10^4$ in length.

Dark halos are identified with a friends-of-friends finder with a linking length of $b=0.164$ in units of the mean-particle separation. We define linked groups with the minimum number of member particles to be 30 as dark halos in the current analysis. We divide those halos (about 1.5×10^6 in total) in five different subgroups according to their mass (table 1) so that each subgroup includes about 3×10^5 halos. Because of the huge size of the AHVS, the number of halos in each subgroup is sufficiently large to characterize the mass dependence of various statistical measures in a reliable manner. In the analysis discussed below, we evaluate the error for each statistical measure from the sample-to-sample variation among the results for eight subboxes (box-size of $1500h^{-1}\text{Mpc}$) constructed out of the entire simulation box.

Table 1. List of five subgroups of dark matter halos in the AHVS.

subgroup	mass range [$h^{-1}M_\odot$]	number of halos
SS	$6.7 \times 10^{13} - 8.0 \times 10^{13}$	328449
S	$8.0 \times 10^{13} - 1.0 \times 10^{14}$	321732
M	$1.0 \times 10^{14} - 1.3 \times 10^{14}$	295204
L	$1.3 \times 10^{14} - 2.0 \times 10^{14}$	300828
LL	$2.0 \times 10^{14} - 6.0 \times 10^{15}$	314782

3. The Nature of Biasing of Dark Halos

First we consider the nonlinear and stochastic nature of halo biasing with particular attention paid to its mass- and scale-dependence. For this purpose, we compute the joint probability distribution function (PDF) of the number density field of halos, δ_{halo} , and the mass density field of dark matter particles, δ_{mass} . Those density fields are first evaluated at 128^3 grids for each subbox data of particles smoothed over a Gaussian radius of R_G . Then, the averaged value of the joint PDF over eight subboxes is computed. Figure 1 shows the averaged joint PDF for specific halo subgroups, LL and SS, at smoothing scales of 30 and $50h^{-1}\text{Mpc}$.

The dotted lines represent the mean biasing, $\overline{\delta_{\text{halo}}}(\delta_{\text{mass}})$, averaged over δ_{halo} at a fixed value of δ_{mass} :

$$\overline{\delta_{\text{halo}}}(\delta_{\text{mass}}) = \int \delta_{\text{halo}} P(\delta_{\text{halo}}|\delta_{\text{mass}}) d\delta_{\text{halo}}. \quad (1)$$

Here, $P(\delta_{\text{halo}}|\delta_{\text{mass}})$ represents the conditional PDF of the halo fields at a given δ_{mass} , which is equal to the joint PDF, $P(\delta_{\text{mass}}, \delta_{\text{halo}})$, divided by the one-point PDF of dark matter, $P(\delta_{\text{mass}})$. We fit the mean biasing to the following quadratic nonlinear model:

$$f_{\text{bias,fit}}(\delta_{\text{mass}}) = b_1 \delta_{\text{mass}} + \frac{b_2}{2} (\delta_{\text{mass}}^2 - \sigma_{\text{mm}}^2), \quad (2)$$

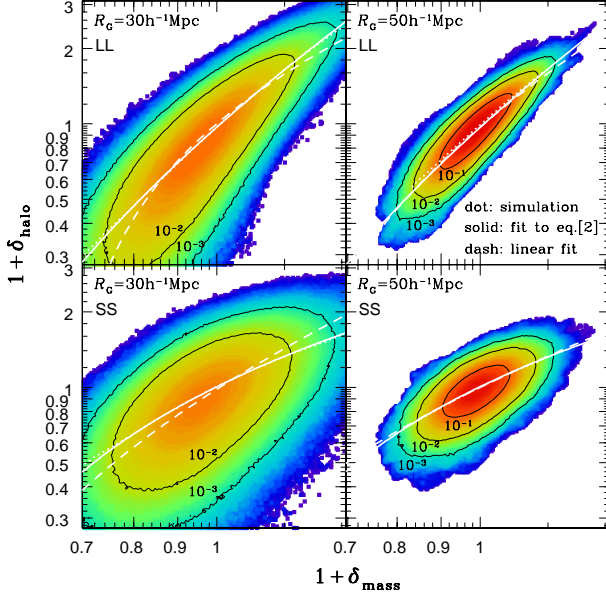


Fig. 1. Joint probability distribution functions, $P(\delta_{\text{mass}}, \delta_{\text{halo}})$, of the halo and the dark matter density fields computed from the Λ HVS data with Gaussian smoothing; *Upper-left*: LL halos with $R_G = 30h^{-1}\text{Mpc}$, *Upper-right*: LL halos with $R_G = 50h^{-1}\text{Mpc}$, *Lower-left*: SS halos with $R_G = 30h^{-1}\text{Mpc}$, *Lower-right*: SS halos with $R_G = 50h^{-1}\text{Mpc}$. Contour lines show $P(\delta_{\text{mass}}, \delta_{\text{halo}}) = 10^{-1}$, 10^{-2} and 10^{-3} . Dotted, dashed and solid lines indicate the mean biasing [equation (1)] and the linear and the quadratic fits [equation (2)] to the mean biasing respectively.

where $\sigma_{\text{mm}} \equiv \langle \delta_{\text{mass}}^2 \rangle^{1/2}$ and $\langle \dots \rangle$ denotes the average over $P(\delta_{\text{mass}})$. The fitted values for the linear and the second-order biasing coefficients, b_1 and b_2 , in each subgroup are listed in table 2. While a linear fit (dashed lines) with $b_2 = 0$ in equation (2) fails to approximate the simulation result, a quadratic fit (solid lines) is quite acceptable for our interest range in the biasing of cluster-scale halos (Hikage et al. 2001).

On the other hand, the stochasticity in the biasing is significantly affected by a shot-noise term in these halo samples due to the small number density of halos. For example, the number of halos within the Gaussian smoothing volume, $(2\pi)^{3/2}R_G^3$ is around 22 at $R_G = 50h^{-1}\text{Mpc}$, and then the shot-noise term amounts to $0.21 (= 1/\sqrt{22})$, which is comparable to the r.m.s. variance listed in table 2. It is, therefore, not easy to extract the information concerning the *pure* stochasticity in the clustering biasing from our halo catalogs. We therefore focus on the non-linear biasing effect and compare the genus for dark halos with perturbative predictions. The effect of the stochasticity of biasing on the halo genus is discussed in appendix 1 using a perturbative analysis.

4. Genus Statistics for Dark Halos in Λ HVS

4.1. Definition and Computing Method of Genus

Genus, $g(\nu_\sigma)$, is defined as $-1/2$ times the Euler characteristic of the isodensity contour of the density field δ

at the threshold level of ν_σ times the r.m.s. fluctuation σ . In practice, this is equal to (number of holes) – (number of isolated regions) of the isodensity surface. In the random-Gaussian field, genus per unit volume is given by the following analytical form:

$$g_{\text{RG}}(\nu_\sigma) = \frac{1}{(2\pi)^2} \left(\frac{\sigma_1^2}{3\sigma^2} \right)^{3/2} (1 - \nu_\sigma^2) \exp\left(-\frac{\nu_\sigma^2}{2}\right), \quad (3)$$

where $\sigma_1 \equiv \langle |\nabla\delta|^2 \rangle^{1/2}$ and $\sigma \equiv \langle \delta^2 \rangle^{1/2}$ ($\nabla\delta$ denotes the spatial derivative of the density field δ and $\langle \dots \rangle$ denotes the average over of the PDF of δ and $\nabla\delta$ (cf., Doroshkevich 1970; Adler 1981; Bardeen et al. 1986; Hamilton et al. 1986)).

In contrast, the genus is often expressed as a function of ν_f instead of ν_σ (e.g., Gott et al. 1989). The threshold ν_f is used to parameterize the fraction f of the volume that lies on the high-density side of the contour,

$$f = \frac{1}{\sqrt{2\pi}} \int_{\nu_f}^{\infty} e^{-x^2/2} dx. \quad (4)$$

Figure 2 shows a comparison between ν_σ and ν_f . The deviation from a linear relation represents the non-Gaussianity of the one-point PDF in the halo field smoothed with scales of 30, 50 and $100h^{-1}\text{Mpc}$ from the left to right panels. While the genus with $R_G = 100h^{-1}\text{Mpc}$ approaches the random-Gaussian prediction, the non-Gaussianity of the one-point PDF is detectable with a smaller R_G and a larger mass of halo. Up to the first order of perturbative correction in σ , the relation between ν_σ and ν_f is given by (Matsubara 2003)

$$\nu_\sigma = \nu_f + \frac{S^{(0)}}{6} (\nu_f^2 - 1) \sigma, \quad (5)$$

where we directly compute a skewness parameter, $S^{(0)} (\equiv \langle \nu_\sigma^3 \rangle / \sigma)$, from the halo field. Figure 2 shows that the lowest order approximation describes the simulated results very accurately at scales of our interest.

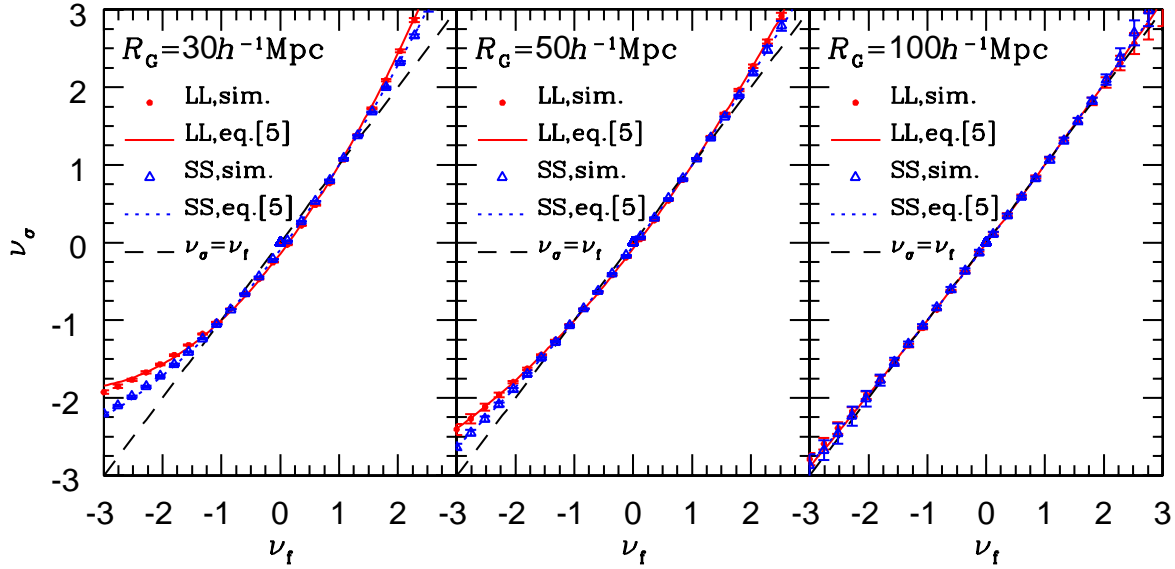
If the evolved density field has an exact one-to-one correspondence with the initial random-Gaussian field, then this transformation from ν_σ to ν_f removes the effect of evolution of the one-point PDF of the density field. Under this assumption, the genus as a function of the volume fraction, expressed as $g(\nu_f)$, is sensitive only to the topology of the isodensity contours, rather than evolution with time of the density threshold assigned to a contour. The limitations of the one-to-one mapping between the initial and evolved density fields are critically examined by Kayo et al. (2001). In the following section, we present the results of the genus in terms of both ν_σ and ν_f .

The computation of genus proceeds as follows: we first assign densities of halos and dark matter particles on 128^3 grids using the cloud-in-cell method. The distance between each grid is sufficiently small so as not to affect the density field smoothed over a scale of $30h^{-1}\text{Mpc}$. The density fields are Fourier-transformed, multiplied by the Gaussian window with a smoothing length of R_G , and then transformed back to a real space. The *smoothed* density fields are used in defining the isodensity surface with a

Table 2. Linear and second-order biasing coefficients.

subgroup	$30h^{-1}\text{Mpc}$			$50h^{-1}\text{Mpc}$			$100h^{-1}\text{Mpc}$		
	b_1^*	b_2^\dagger	σ^\ddagger	b_1^*	b_2^\dagger	σ^\ddagger	b_1^*	b_2^\dagger	σ^\ddagger
SS	1.69	$-0.72(\pm 0.05)$	0.32	1.66	$-0.69(\pm 0.13)$	0.16	1.63	$1.50(\pm 1.18)$	0.06
S	1.76	$-0.60(\pm 0.04)$	0.33	1.76	$-0.76(\pm 0.14)$	0.16	1.72	$-0.24(\pm 1.18)$	0.06
M	1.88	$-0.31(\pm 0.04)$	0.35	1.87	$-0.53(\pm 0.15)$	0.17	1.88	$-1.95(\pm 1.05)$	0.06
L	2.16	$0.38(\pm 0.05)$	0.36	2.12	$-0.27(\pm 0.16)$	0.18	2.05	$-0.40(\pm 1.08)$	0.06
LL	2.94	$4.37(\pm 0.03)$	0.42	2.97	$4.48(\pm 0.11)$	0.21	3.05	$1.59(\pm 0.96)$	0.07

* Linear biasing coefficients.

 † Second-order biasing coefficients with 1σ fitting error[equation (2)]. ‡ the amplitude of the rms density fluctuation of halos $\sigma \equiv \langle \delta_{\text{halo}}^2 \rangle^{1/2}$ with Gaussian smoothing.**Fig. 2.** Comparison between ν_f and ν_σ directly computed from the density fields of LL (filled circles) and SS (open triangles) halo subgroups with sample-to-sample variations. The perturbative expression up to the first order of σ [equation (5)] is also plotted for the LL subgroup (solid lines) and the SS subgroup (dotted lines). From left to right, Gaussian smoothing scale is 30, 50, and $100h^{-1}\text{Mpc}$, respectively. The dashed lines indicate the linear relation.

given threshold, and the resulting genus is evaluated with the CONTOUR 3D code (Weinberg 1988) by integrating the deficit angles over the isodensity surface.

4.2. Genus Statistics for Dark Matter and Dark Halos

Since the one-point PDF of dark matter particles is empirically known to be well approximated by the log-normal PDF (e.g. Coles, Jones 1991; Kofman et al. 1994; Kayo et al. 2001), it is natural to expect that it is also the case for genus. In fact, Matsubara and Yokoyama (1996) derived a genus expression for dark matter assuming the nonlinear density field of dark matter has a one-to-one mapping to its primordial Gaussian field. If one adopts the log-normal mapping, their result can be explicitly written as

$$g_{\text{LN}}(\nu_\sigma) = g_{\text{MAX,LN}}[1 - x_{\text{LN}}^2(\nu_\sigma)] \exp\left[-\frac{x_{\text{LN}}^2(\nu_\sigma)}{2}\right], \quad (6)$$

$$x_{\text{LN}}(\nu_\sigma) \equiv \frac{\ln[(1 + \nu_\sigma \sigma)\sqrt{1 + \sigma^2}]}{\sqrt{\ln(1 + \sigma^2)}}, \quad (7)$$

where the maximum value, $g_{\text{MAX,LN}}$ is defined by

$$g_{\text{MAX,LN}} = \frac{1}{(2\pi)^2} \left[\frac{\sigma_1^2}{3(1 + \sigma^2)\ln(1 + \sigma^2)} \right]^{3/2}. \quad (8)$$

Note that g_{LN} in terms of ν_f just reduces to the Gaussian prediction (3). In reality, this one-to-one mapping assumption is much stronger than the statement that the one-point PDF is empirically well approximated by the log-normal PDF.

We compare the genus for dark matter averaged over eight sub-boxes with the analytical expressions [equations (3) and (6)] multiplied by the volume of the sub-boxes, $(1500h^{-1}\text{Mpc})^3$. The calculations of σ and σ_1 in the analytical predictions are based on the power spectrum by Peacock and Dodds (1996). Figure 3 shows that genus as a function of ν_σ [panel (a)], the difference, between the genus for the simulated dark matter g_{DM} and the analytical predictions g_{theory} , normalized by the maximum value of g_{DM} , $g_{\text{MAX,DM}}$ [panel (b)], and the same as panels (a) and (b), but as a function of ν_f [panels (c) and (d)].

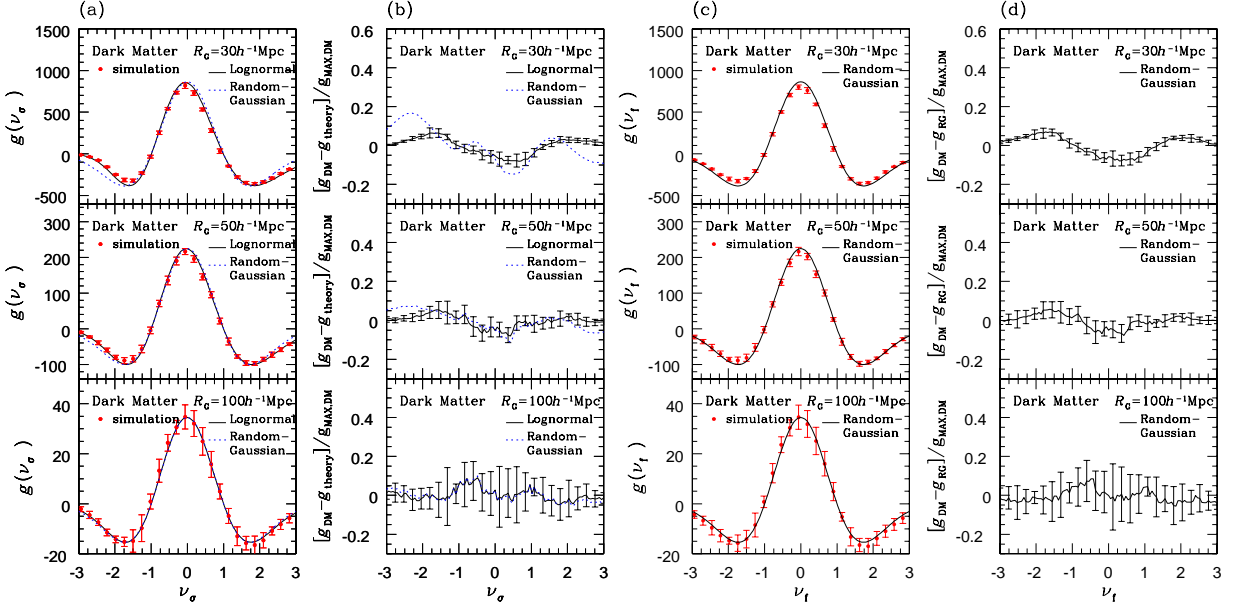


Fig. 3. Panel (a): Genus for dark matter computed from AHVS with filled circles and the analytical genus expression in random-Gaussian with dotted lines [equation (3)] and in log-normal statistics with solid lines [equation (6)]. The top, middle, and bottom panels, respectively, indicate the results for smoothing lengths of $30h^{-1}\text{Mpc}$, $50h^{-1}\text{Mpc}$, and $100h^{-1}\text{Mpc}$. This order of the smoothing scale is the same in the other panels. Panel (b): The difference between our simulation results (denoted by g_{DM}) and the theoretical predictions (denoted by g_{theory} ; the random-Gaussian expression with dotted lines, the log-normal model with solid lines containing error-bars) normalized by the amplitude of the simulated genus (denoted by $g_{\text{MAX,DM}}$). Panels (c) and (d): Same as panels (a) and (b), but for genus as a function of ν_f [equation (4)]. The simulated results are compared with the random-Gaussian expression with error-bars (denoted by g_{RG})

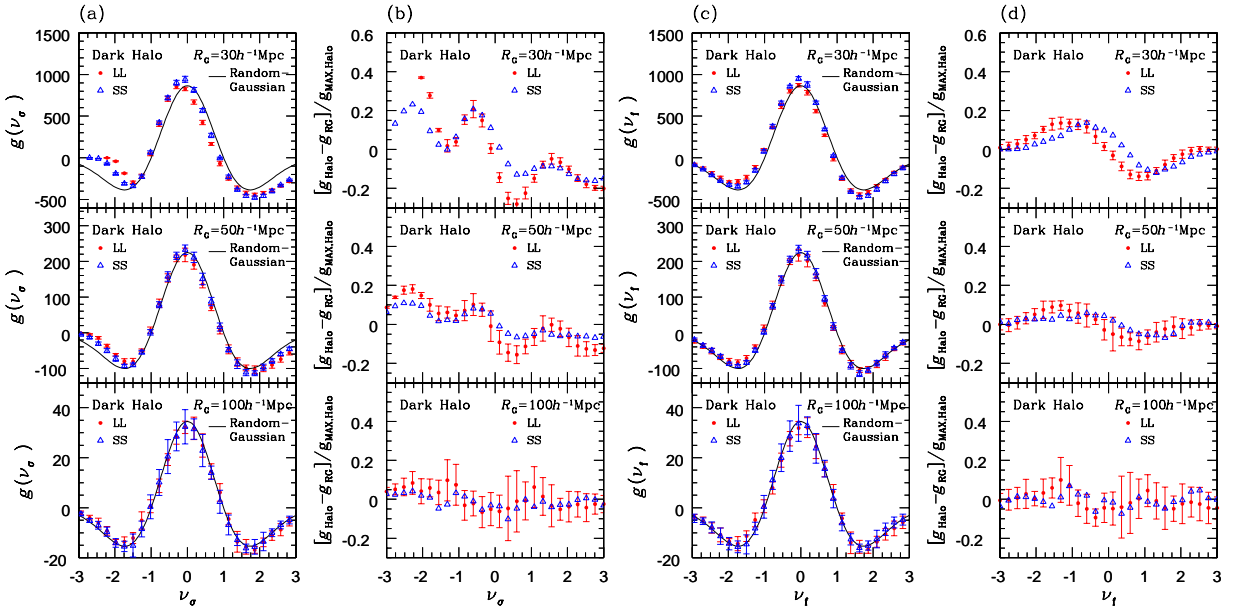


Fig. 4. Same as figure 3 but for dark halos in LL (filled circles) and SS (open triangles) subgroups. The sample-to-sample variance of genus is plotted with error-bars only for the LL subgroup. Panels (a) and (b): Comparison between the genus for halos (denoted by g_{Halo}) with the simulated genus for dark matter (denoted by g_{DM}) as a function of ν_σ . Panels (c) and (d): Comparison between genus for halos as a function of ν_f with equation (3).

We estimate the sample-to-sample variance of the simulated genus $\Delta g(\nu)$ by

$$\Delta g(\nu) = \left\{ \sum_{i=1}^8 [g_i(\nu) - \bar{g}(\nu)]^2 / 7 \right\}^{1/2}, \quad (9)$$

where $g_i(\nu)$ denotes the value of the genus on the contour surface at the threshold ν estimated from sub-box i ; $\bar{g}(\nu)$ is the value of the genus averaged over eight sub-boxes.

Panels (a) and (b) show that the empirical prediction (6) well explains our current results for dark matter including both the amplitude and the shape of the genus in our interested scale. This is consistent with the numerical results by Matsubara and Yokoyama (1996). Panels (c) and (d) show that the genus for dark matter as a function of ν_f agrees with the analytical prediction for a Gaussian random field [equation (3)].

We then plot the genus for dark halos of two specific subgroups, LL and SS in figure 4. While panels (a) and (b) show comparisons of the halo genus with the simulated genus for mass as a function of ν_σ , the panels (c) and (d) represent the results in terms of ν_f . The differences in the genus for halos from the simulated genus for dark matter [panel (b)] or the random-Gaussian prediction [panel (d)] are normalized by the maximum value of the genus for halos, $g_{\text{MAX, Halo}}$. Figure 4 shows that the non-Gaussianity induced by halo biasing is comparable to that by the non-linear gravitational evolution, and that the shape and the amplitude of the halo genus are almost insensitive to the halo mass. The result suggests that the influence of biasing can be corrected perturbatively. To see the weak dependence of the genus on the halo mass more clearly, we plot in figure 5 the ratio of the genus amplitude, $g_{\text{MAX, Halo}}/g_{\text{MAX, DM}}$, i.e., the maximum value of the genus amplitude for dark halos divided by that for dark matter. The results for each halo subgroup are plotted as a function of the averaged halo mass. While the increase of the smoothing scale significantly changes the genus amplitude in figure 4, the relative amplitude in figure 5 almost remains unchanged for a wide range of the halo mass. Furthermore, the amplitude of halo genus is very close to that of dark matter, with only 6 – 16 percent deviations at $R_G = 30 h^{-1} \text{Mpc}$. This is indeed consistent with the prediction of Hikage et al. (2001) based on the one-to-one mapping assumption from the genus for dark matter. Therefore, one can conclude that the biasing effect on halo genus on the cluster-mass scale is generally small, and that the perturbative analysis based on Edgeworth formula is safely applicable at $R_G \geq 30 h^{-1} \text{Mpc}$.

4.3. Comparison with Perturbation Theory

Having established the weak influence of the biasing, we wish to further examine the halo genus for a better understanding of the nature of biasing. For this purpose, we attempt to model the halo genus using a perturbative approach with particular emphasis on the nonlinearity of the biasing effect. We start with Matsubara's expression for the genus density in a weakly non-Gaussian field (Matsubara 1994, 2003). In the lowest-order approxima-

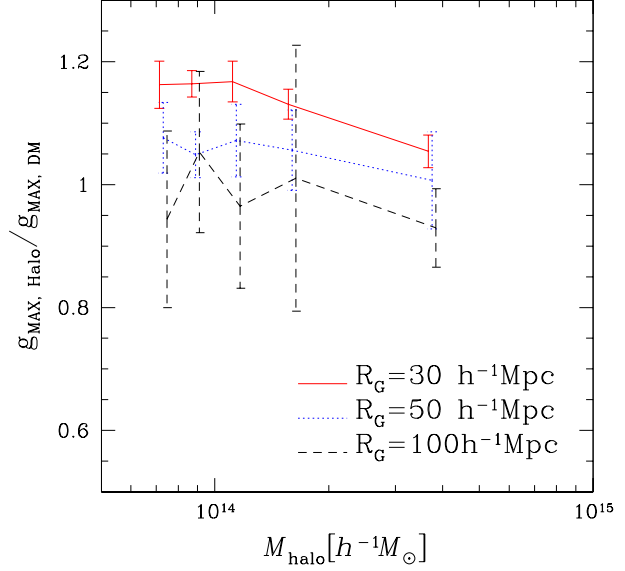


Fig. 5. Ratio of the amplitude of genus for halos, $g_{\text{MAX, Halo}}$, to that for dark matter, $g_{\text{MAX, DM}}$ as a function of the mean halo mass for each subgroup. The smoothing scale R_G is 30 (solid), 50 (dotted), and $100 h^{-1} \text{Mpc}$ (dashed).

tion, his result reduces to

$$g_{\text{PT}}(\nu_\sigma) = -\frac{1}{(2\pi)^2} \left(\frac{\sigma_1^2}{3\sigma^2} \right)^{\frac{3}{2}} \exp\left(-\frac{\nu_\sigma^2}{2}\right) \left\{ H_2(\nu_\sigma) + \left[\frac{S^{(0)}}{6} H_5(\nu_\sigma) + S^{(1)} H_3(\nu_\sigma) + S^{(2)} H_1(\nu_\sigma) \right] \sigma \right\}, \quad (10)$$

where $H_n(\nu_\sigma)$ are the Hermite polynomials and $S^{(n)}$ represent the skewness parameters, defined as

$$S^{(0)} = \frac{\langle \nu_\sigma^3 \rangle}{\sigma}, \quad S^{(1)} = -\frac{3}{4} \frac{\langle \nu_\sigma^2 (\nabla^2 \nu_\sigma) \rangle \sigma}{\sigma_1^2}, \quad S^{(2)} = -\frac{9}{4} \frac{\langle (\nabla \nu_\sigma \cdot \nabla \nu_\sigma) (\nabla^2 \nu_\sigma) \rangle \sigma^3}{\sigma_1^4}. \quad (11)$$

With the relation between ν_σ and ν_f [equation (5)], the genus as a function of ν_f is rewritten by

$$g_{\text{PT}}(\nu_f) = -\frac{1}{(2\pi)^2} \left(\frac{\sigma_1^2}{3\sigma^2} \right)^{\frac{3}{2}} \exp\left(-\frac{\nu_f^2}{2}\right) \left\{ H_2(\nu_f) + \left[(S^{(1)} - S^{(0)}) H_3(\nu_f) + (S^{(2)} - S^{(0)}) H_1(\nu_f) \right] \sigma \right\}. \quad (12)$$

In the case of weak non-Gaussianity induced by the non-linear gravitational evolution, the above expression proves to be in good agreement with the genus computed from the earlier N-body simulation data (Matsubara, Suto 1996; Matsubara, Yokoyama 1996). We extend those previous studies and examine whether or not equations (10) and (12) are also applicable to the weak non-Gaussianity induced by the halo biasing (in addition to the nonlinear gravitational evolution).

Figure 6 represents a comparison between the simulated results for the most strongly biased halo subgroup LL and the perturbative model of genus as a function of ν_σ in

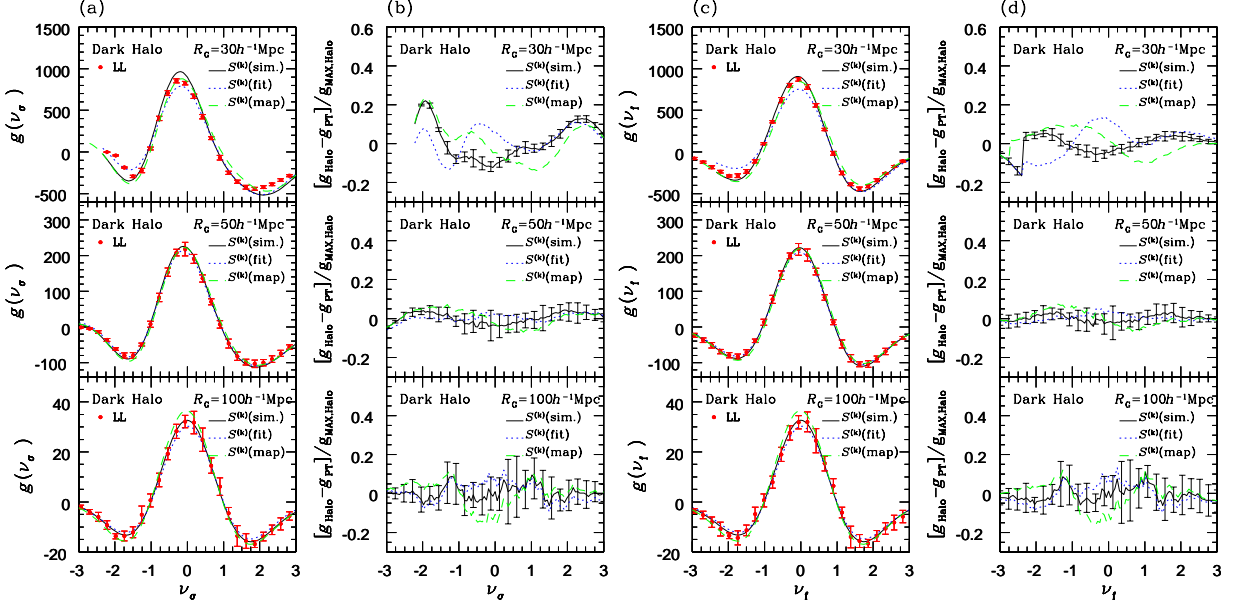


Fig. 6. Same as figure 4, but for a comparison of the simulated genus for LL halos (denoted by g_{Halo}) with the second-order perturbative formula [equation (10)] (denoted by g_{PT}). The skewness parameters in the perturbative formula are calculated in the following three ways: (i) a direct computation from the simulated halo density field (solid, labeled by ‘sim.’), (ii) fitting of the simulated halo genus to the perturbative formula with skewness parameters put as free parameters (dotted, labeled by ‘fit’), and (iii) direct computation from the δ_{halo} field obtained by one-to-one mapping from the dark matter field with the simulated mean biasing (dashed, labeled by ‘map’). The error-bars, which indicate the sample-to-sample variance [equation(9)], are plotted only for the genus with skewness parameters calculated by (i).

panels (a) and (b) and of ν_f in panels (c) and (d). We explicitly show the differences between the simulation results, g_{Halo} , and the prediction of the perturbative model, g_{PT} , divided by the amplitude of the simulated genus, $g_{\text{MAX,Halo}}$, in panel (b) for $g(\nu_\sigma)$ and panel (d) for $g(\nu_f)$. For the prediction of the perturbative model in equations (10) and (12), the r.m.s. fluctuation of the halo density field, $\sigma = \langle \delta_{\text{halo}}^2 \rangle^{1/2}$, and that of its first spatial derivative field, $\sigma_1 = \langle |\nabla \delta_{\text{halo}}|^2 \rangle^{1/2}$, are computed directly from the halo density field. We compute the skewness parameters $S^{(0)}$, $S^{(1)}$, and $S^{(2)}$ using three different methods: (i) a direct computation from the halo density field (labeled by ‘sim.’), (ii) fitting of our simulated genus to the perturbative formula as free parameters (labeled by ‘fit’), and (iii) a direct computation from the δ_{halo} field (labeled by ‘map’), based on one-to-one mapping [equation (1)], assuming the nonlinear deterministic biasing. For computations of (i) and (iii), the gradient and Laplacian values of the density fields in equation (11) are evaluated by making the corresponding spatial derivative in Fourier space, respectively. As for (ii), the range of the fitting is restricted from $\nu_\sigma = \text{Max}(-1/\sigma, -2.5)$ to $\nu_\sigma = 2.5$.

Figure 6 shows that the perturbative formula [equation (10)] is valid for the halo genus at $R_c \geq 50h^{-1}\text{Mpc}$. The approximation by the perturbative formula is also good in $|\nu| \leq 1.5$ at $R_c = 30h^{-1}\text{Mpc}$, although the large deviation in $|\nu| \geq 1.5$ might be attributed to the limitation of the Edgeworth expansion, which is also seen in the dark matter case (Matsubara and Suto 1996). The difficulty to distinguish the perturbative prediction using the δ_{halo}

field from other genus implies that the biasing effect on the halo genus is well approximated by nonlinear deterministic biasing.

Next, we examine whether or not one can reproduce the best-fit values for those skewness parameters from the independent theoretical models and/or simulation data. Figure 7 plots the skewness parameters calculated from the above three methods. A weak dependence of the skewness parameters on the halo mass is consistent with a model prediction by Mo et al. (1997). Fitting method (ii) reproduces the skewness parameters well at a smoothing scale of $50h^{-1}\text{Mpc}$, while the approximation by the perturbative formula breaks down on the scale of $30h^{-1}\text{Mpc}$, especially for the $S^{(2)}$ term. It is almost impossible to reproduce skewness parameters accurately at a smoothing scale of $100h^{-1}\text{Mpc}$, because the statistical error is large due to the small value of the genus.

A good agreement of the skewness parameters from the δ_{halo} field again suggests that the approximation by the nonlinear deterministic biasing works well in the halo genus over the cluster-mass scales. Recalling the fact that the nonlinearity in the halo biasing is well described by the linear and the quadratic terms shown in section 3, an accurate prediction of the halo genus is feasible from appropriate modeling of the two biasing coefficients. The reason why the stochastic effect of the biasing is nearly negligible can be understood from the fact that the stochastic components are almost cancelled out by each other in the form of skewness parameters (see appendix 1).

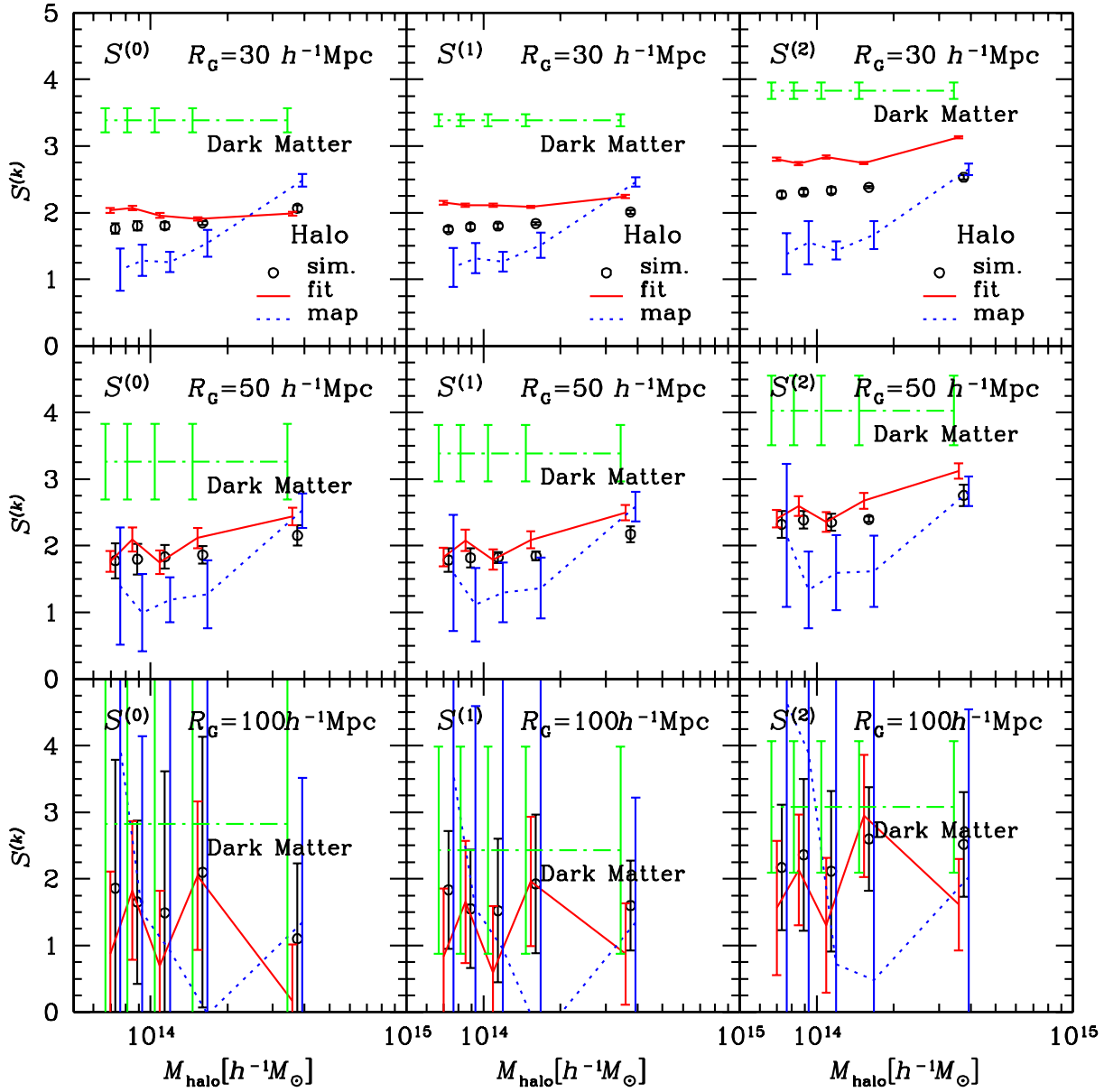


Fig. 7. Skewness parameters, $S^{(0)}$ (left), $S^{(1)}$ (middle) and $S^{(2)}$ (right) as a function of halo mass averaged over each subgroup with $R_G = 30h^{-1}\text{Mpc}$ (top), $R_G = 50h^{-1}\text{Mpc}$ (middle) and $R_G = 100h^{-1}\text{Mpc}$ (bottom). Labels of 'sim.', 'fit' and 'map' have the same meanings as figure 6. Dashed lines indicate skewness parameters for the dark matter field. The horizontal position of each plot is slightly staggered for easy view.

5. Conclusions

We evaluate the extent to which halo biasing affects the genus for dark halos of cluster-scale mass using the Hubble volume simulations. The huge volume of the data enables us to perform the most reliable systematic analysis of the genus for dark halos and to calculate the sample-to-sample error corresponding to the cosmic variance. Through a detailed comparison of the genus for dark halos with that for the mass distribution, we find that the non-Gaussianity induced by the biasing is comparable to that by the nonlinear gravitational evolution. To characterize the biasing effect on the genus for dark halos, we extensively apply a perturbative formula developed by Matsubara (1994). We find that the perturbative formula is indeed very accurate for the genus of dark halos at a smoothing length of $R_G \geq 50h^{-1}\text{Mpc}$. The skewness parameters obtained from a fitting of the perturbative formula consistently reproduce the results directly measured from the density field. We also find that the nonlinear deterministic biasing well describes the biasing effect on the genus for dark halos. Moreover, the nonlinearity of biasing can be approximated by only the linear and quadratic terms. A prediction of genus for the dark halo on the cluster-scale mass scale is thus possible from an appropriate modeling of these two parameters.

Our results show that the contribution of biasing stochasticity to the genus statistics is very small at $R \geq 30h^{-1}\text{Mpc}$ and that the dependence of the halo mass is safely negligible within the sampling error-bars. On the other hand, both the non-linearity of the biasing and the gravitational evolution alter the shape of the genus, depending on the smoothing scale. In a weakly nonlinear regime, one can even discriminate these two effects using perturbative theory. In light of this, our formulation, including the nonlinearity of biasing and gravitational evolution in a previous paper (Hikage et al. 2001), may provide a theoretical guide for characterizing the real observational data. At the current observational level, however, the above biasing effect is very difficult to detect because the biasing effect on the genus is small even in a much larger volume size of $(1500h^{-1}\text{Mpc})^3$, as shown in figure 4. The other observational effects, including the redshift distortion and the light-cone effect, are also small in the present observational status (Matsubara, Suto 1996; Colley et al. 2000). Therefore, the initial Gaussianity can be probed directly by the genus from the upcoming galaxy cluster catalogs within the sampling errors.

We thank the referee, David Weinberg, for a critical reading and useful comments. We also thank Naoki Yoshida for providing the dark matter and halo density fields from the Hubble Volume simulation and for useful comments and Y. Ohta for providing his program to make contour plots. Numerical computations were carried out at ADAC (the Astronomical Data Analysis Center) of the National Astronomical Observatory, Japan (project ID:mys02) and at KEK (High Energy Accelerator Research Organization, Japan). One of us (A.T.) ac-

knowledges the support by the Grant-in-Aid for Scientific Research for JSPS (No. 1470157). This research was supported in part by the Grant-in-Aid by the Ministry of Education, Culture, Sports, Science and Technology of Japan (07CE2002, 12640231) to RESCEU, and by the Supercomputer Project (No.99-52, N0.00-63) of KEK.

References

- Adler, R.J. 1981, *The Geometry of Random Fields* (Chichester: Wiley)
- Bardeen, J. M., Bond, J. R., Kaiser, N., & Szalay, A. S. 1986, *ApJ*, 304, 15
- Blanton, M., Cen, R., Ostriker, J. P., & Strauss, M. A. 1999, *ApJ*, 522, 590
- Canavezes, A., et al. 1998, *MNRAS*, 297, 777
- Colberg, J. M., et al. 2000, *MNRAS*, 319, 209
- Coles, P., & Jones, B. 1991, *MNRAS*, 248, 1
- Colley, W. N., Gott, J. R., III, Weinberg, D. H., Park, C., & Berlind, A. A. 2000, *ApJ*, 529, 795
- Dekel, A., & Lahav, O. 1999, *ApJ*, 520, 24
- Doroshkevich, A. G. 1970, *Astrofizika*, 6, 581 (English transl. *Astrophysics*, 6, 320)
- Eke, V. R., Cole, S., & Frenk, C. S. 1996, *MNRAS*, 282, 263
- Fry, J. N., & Gaztañaga, E. 1993, *ApJ*, 413, 447
- Gott, J. R., III, Mellot, A. L., & Dickinson, M. 1986, *ApJ*, 306, 341
- Gott, J. R., III, et al. 1989, *ApJ*, 340, 625
- Hamana, T., Yoshida, N., Suto, Y., & Evrard, A.E. 2001, *ApJ*, 561, L143
- Hamilton, A. J. S., Gott, J. R., III, & Weinberg, D. H. 1986, *ApJ*, 309, 1
- Hikage, C., Taruya, A., & Suto, Y. 2001, *ApJ*, 556, 641
- Hikage, C., Suto, Y., Kayo, I., Taruya, A., Matsubara, T., Vogeley, M. S., Hoyle, F., Gott, J. R., III, Brinkmann, J., for the SDSS collaboration 2002, *PASJ*, 54, 707
- Hoyle, F., Vogeley, M. S., Gott, J. R., III, Blanton, M., Tegmark, M., Weinberg, D. H., Bahcall, N., Brinkmann, J., & York, D. G. for the SDSS collaboration 2002, *ApJ*, 580, 663
- Jenkins, A., Frenk, C. S., White, S. D. M., Colberg, J. M., Cole, S., Evrard, A. E., Couchman, H. M. P., & Yoshida, N. 2001, *MNRAS*, 321, 372
- Kaiser, N. 1984, *ApJ*, 284, L9
- Kayo, I., Taruya, A., & Suto, Y. 2001, *ApJ*, 561, 22
- Kitayama, T., & Suto, Y. 1997, *ApJ*, 490, 557
- Kofman, L., Bertschinger, E., Gelb, J. M., Nusser, A., & Dekel, A. 1994, *ApJ*, 420, 44
- Matsubara, T. 1994, *ApJ*, 434, L43
- Matsubara, T., & Yokoyama, J. 1996, *ApJ*, 463, 409
- Matsubara, T., & Suto, Y. 1996, *ApJ*, 460, 51
- Matsubara, T. 2003, *ApJ*, in press (astro-ph/0006269)
- Mo, H., Jing, Y. P., & White, S. D. M. 1997, *MNRAS*, 284, 189
- Mo, H., & White, S. D. M. 1996, *MNRAS*, 282, 347
- Moore, B., Frenk, C. S., Weinberg, D. H., Saunders, W., Lawrence, A., Ellis, R. S., Kaiser, N., Efstathiou, G., & Rowan-Robinson, M. 1992, *MNRAS*, 256, 477
- Park, C., Gott, J. R., III, & da Costa, L. N. 1992, *ApJ*, 392, L51
- Peacock, J. A., & Dodds, S. J. 1996, *MNRAS*, 280, L19
- Rhoads, J. E., Gott, J. R., III, & Postman, M. 1994, *ApJ*, 421, 1

Seto, N., Yokoyama, J., Matsubara, T., & Siino, M. 1997, ApJS, 110, 177

Somerville, R. S., Lemson, G., Sigrad, Y., Dekel, A., Kauffmann, G., & White, S. D. M. 2001, MNRAS, 320, 289

Taruya, A., & Suto, Y. 2000, ApJ, 542, 559

Taruya, A., Magira, H., Jing, Y. P., & Suto, Y. 2001, PASJ, 53, 155

Vogele, M. S., Park, C., Geller, M. J., Huchra, J. P., & Gott, J. R., III 1994, ApJ, 420, 525

Yoshikawa, K., Taruya, A., Jing, Y. P., & Suto, Y. 2001, ApJ, 558, 520

Watanabe, T., Matsubara, T., & Suto, Y. 1994, ApJ, 432, 17

Weinberg, D. H. 1988, PASP, 100, 1373

Appendix 1. Influence of Biasing Stochasticity in a Weakly Nonlinear Regime

In this appendix, we discuss the influence of biasing stochasticity on the halo genus in a weakly nonlinear regime. For this purpose, based on the perturbative formula by Matsubara (1994) [equations (10) and (11)], we evaluate the skewness parameters. Suppose that the halo density field is split into the deterministic and the residual stochastic terms;

$$\delta_{\text{halo}} = \overline{\delta_{\text{halo}}} + s_{\text{halo}}, \quad (\text{A1})$$

where the mean deterministic term is formally defined by

$$\overline{\delta_{\text{halo}}}(\delta_{\text{mass}}) = \int \delta_{\text{halo}} P(\delta_{\text{halo}}|\delta_{\text{mass}}) d\delta_{\text{halo}}, \quad (\text{A2})$$

in terms of the conditional PDF of the halo fields at a given δ_{mass} . Note that equation (A1) implies that $\langle s_{\text{halo}} F(\delta_{\text{mass}}) \rangle = 0$ for any function $F(\delta_{\text{mass}})$ because of the relation $\langle \delta_{\text{halo}} F(\delta_{\text{mass}}) \rangle = \langle \overline{\delta_{\text{halo}}} F(\delta_{\text{mass}}) \rangle$.

In a weakly nonlinear regime of the dark matter density field, the nonlinearity in the biasing may be well approximated by the following quadratic form:

$$\overline{\delta_{\text{halo}}}(\delta_{\text{mass}}) = b_1 \delta_{\text{mass}} + \frac{b_2}{2} (\delta_{\text{mass}}^2 - \sigma_{\text{mm}}^2) + \dots, \quad (\text{A3})$$

with the quantity σ_{mm}^2 being $\langle \delta_{\text{mass}}^2 \rangle$. In this case, the variance of the halo and the covariance of the halo and dark matter are evaluated as follows:

$$\sigma_{\text{hh}}^2 \equiv \langle \delta_{\text{halo}}^2 \rangle \approx b_1^2 \sigma_{\text{mm}}^2 + \langle s_{\text{halo}}^2 \rangle, \quad (\text{A4})$$

$$\sigma_{\text{hm}}^2 \equiv \langle \delta_{\text{halo}} \delta_{\text{mass}} \rangle \approx b_1 \sigma_{\text{mm}}^2. \quad (\text{A5})$$

The above results can be translated to the skewness of the halo density field as

$$\langle \delta_{\text{halo}}^3 \rangle \approx b_1^3 \sigma_{\text{mm}}^4 \left(S_{\text{m}}^{(0)} + 3 \frac{b_2}{b_1} + \frac{3b_1 \langle s_{\text{halo}}^2 \delta_{\text{mass}} \rangle + \langle s_{\text{halo}}^3 \rangle}{b_1^3 \sigma_{\text{mm}}^4} \right), \quad (\text{A6})$$

where the quantity $S_{\text{m}}^{(0)}$ means the skewness of the mass density field, $S_{\text{m}}^{(0)} \equiv \langle \delta_{\text{mass}}^3 \rangle / \sigma_{\text{mm}}^4$. Then, one obtains an expression for the normalized skewness, $S_{\text{h}}^{(0)}$, for the halo density field as

$$S_{\text{h}}^{(0)} \equiv \frac{\langle \delta_{\text{halo}}^3 \rangle}{\sigma_{\text{hh}}^4} \approx \frac{1}{b_1} \left(S_{\text{m}}^{(0)} + 3 \frac{b_2}{b_1} + \frac{3b_1 \langle s_{\text{halo}}^2 \delta_{\text{mass}} \rangle + \langle s_{\text{halo}}^3 \rangle}{b_1^3 \sigma_{\text{mm}}^4} \right) (1 + \epsilon_{\text{scatt}}^2)^{-2}, \quad (\text{A7})$$

where we adopt a measure for the stochasticity of biasing, ϵ_{scatt} (Dekel, Lahav 1999; Taruya, Suto 2000),

$$\epsilon_{\text{scatt}}^2 \equiv \frac{\sigma_{\text{mm}}^2 \langle s_{\text{halo}}^2 \rangle}{\sigma_{\text{hm}}^4} \approx \frac{1}{b_1^2} \frac{\langle s_{\text{halo}}^2 \rangle}{\sigma_{\text{mm}}^2}. \quad (\text{A8})$$

In deriving the above results, we did not treat the stochastic term, s_{halo} , as a small quantity, which might not be guaranteed even in a weakly nonlinear regime.

Equation (A7) is a natural extension of the frequently used expression within the framework of deterministic nonlinear biasing (e.g., Fry, Gaztañaga 1993);

$$S_{\text{h}}^{(0)} = \frac{1}{b_1} \left(S_{\text{m}}^{(0)} + 3 \frac{b_2}{b_1} \right), \quad (\text{A9})$$

which is only valid in absence of stochasticity, $s_{\text{halo}} = 0$. Compared (A7) with (A9), we readily see the role of stochasticity to the skewness parameter as follows: while the width of scatter, ϵ_{scatt} , decreases the skewness amplitude, non-Gaussianity characterized by the third order moments, $\langle s_{\text{halo}}^2 \delta_{\text{mass}} \rangle$ and $\langle s_{\text{halo}}^3 \rangle$ conversely increases the overall amplitude. Indeed, this fact illustrates the general trend of the skewness parameters. That is, the skewness parameters can be schematically divided into the contributions from nonlinearity and stochasticity of biasing as follows:

$$S_{\text{h}}^{(n)} = \frac{1}{b_1} \frac{\left(S_{\text{m}}^{(n)} + 3 \frac{b_2}{b_1} + [\text{3rd order stochasticity}] \right)}{(1 + [\text{2nd order stochasticity}])}, \quad (\text{A10})$$

where the third order stochasticity characterizes the non-Gaussianity induced by the stochasticity of biasing and the second order stochasticity represents the degree of stochasticity.

Equation (A10) illustrates the qualitative behavior of the normalized skewness for the halo field: (i) it is inversely proportional to the linear bias coefficient b_1 , (ii) the nonlinearity (with $b_2 > 0$) *increases* the skewness, and (iii) the stochasticity *decreases* the overall amplitude of the skewness, but adds a positive term to the purely gravitational term S_{m} . Although it is not clear which of the two opposite effects due to the stochasticity is more important, the results in figures 6 and 7 show that total stochastic effect is not very strong as far as those skewness parameters are concerned. This indicates that two opposite effects due to the biasing stochasticity on the skewness parameters [equation (A10)] are almost cancelled out by each other.